Macromolecules

pubs.acs.org/Macromolecules Article

Stretchable Sponge-like Hydrogels with a Unique Colloidal Network Produced by Polymerization-Induced Microphase Separation

Xin Ning Zhang, Cong Du, Zhou Wei, Miao Du, Qiang Zheng, and Zi Liang Wu*

Cite This: https://doi.org/10.1021/acs.macromol.1c02129 Read Online

ACCESS | Metrics & More | Article Recommendations | Supporting Information

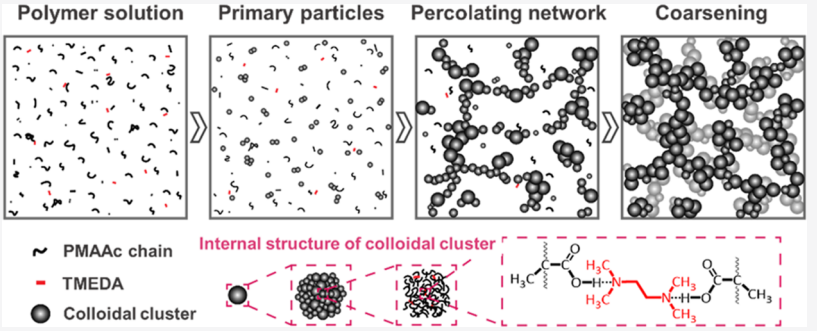

ABSTRACT: We report a series of sponge-like hydrogels prepared by polymerizing an aqueous solution of methacrylic acid (MAAc) in the presence of *N*,*N*,*N*′,*N*′-tetramethylethylenediamine (TMEDA), which results in hydrogen bond complexation, microphase separation, and formation of a unique colloidal network. The microstructure of the gels is determined by the coupling of microphase separation and gelation, which are influenced by the feeding concentrations of MAAc and TMEDA. Colloidal gels are only obtained at a relatively low concentration of MAAc in the presence of a certain amount of TMEDA. The structural evolution during the polymerization and the formation mechanism for the colloidal network are revealed by a combination of dynamic light scattering measurements and optical microscopy. It reveals that hydrogen bond complexes are formed between poly(methacrylic acid) (PMAAc) and TMEDA, leading to the formation of colloidal particles that assemble into clusters and then the interconnected colloidal network. The physical hydrogels with a colloidal network are stable in water and possess high stretchability and good self-recovery ability due to the robustness of colloidal particles joined by adhesive PMAAc chains. These sponge-like hydrogels are applied to remove dye molecules for water purification and devised into a solar vapor generation device to produce clean water. The strategy by harnessing reaction-induced phase separation should be applicable for other systems to engineering the microstructure and properties of functional materials toward specific applications.

INTRODUCTION

Colloidal gels are one class of soft matters with unique microstructures and functionalities, which usually consist of an interconnected solid particle network and the filled liquid solvent. The unique structural characteristic endows colloidal gels with versatile applications in the food industry, tissue engineering scaffolds, building materials, etc.[1−7] Self-assembly and phase separation are two essential strategies for the development of colloidal aggregates, during which, locally, dynamical arrest or jamming occurs by strong attractive or repulsive interactions between polymer chains and/or particles that can be regulated by variations of environmental conditions.[1−4,8−18] For example, in the manufacture of acidified milk products (yogurt, cheese, etc.), the decrease in pH disrupted the stabilized surface layer of κ-casein micelles, resulting in collapse and aggregation of the particles and thus gelation to form a colloidal network.[2] Tanaka and co-workers investigated this process in a steric- and charge-stabilized colloidal suspension; the introduction of salt led to an electrostatic screening of electrostatic repulsion between the colloids that aggregated to form a colloidal network.[9] However, these colloidal networks have poor mechanical properties and cannot maintain the structural morphology over a long period of time due to the relatively weak interaction between colloidal particles, which hinders the potential applications as soft materials in biomedical and engineering fields.

In recent years, noncovalent interactions and their associations between polymer chains are used for the development of tough supramolecular hydrogels.[19−24] Mechanically robust hydrogels with a colloidal network should be produced by enhancing the connection and interaction

Received: October 12, 2021
Revised: November 25, 2021

between the colloidal particles.[25−27] For instance, micron-sized aggregates were obtained by Zhu et al. after mixing aqueous solutions of oppositely charged polyelectrolytes.[25] The precipitates settled down and assembled into a robust bulk hydrogel with a colloidal network by forming ionic bonds between the polyion complex colloids. Besides the physical gelation process, gel materials are usually prepared by chemical reactions such as polymerization of precursor solutions. Microporous hydrogels are synthesized by polymerization-induced phase separation, while hydrogels with a colloidal network are rarely developed.[28,29] This is because the reaction usually results in spinodal phase separation that produces hydrogels with a bicontinuous structure.[30,31] It remains a big challenge to tailor the phase separation process so as to form colloidal aggregates and then assemble into a colloidal network during the polymerization of a homogeneous precursor solution.[32−36] However, various polymer aerogels with a colloidal network structure have been developed by polymerization-induced phase separation.[35] The poor solubility of reaction-produced polymers results in the formation of compact colloidal particles in organic solvent that assemble into a colloidal network during the following reaction process. During the polymerization, phase separation and gelation compete with each other, and the kinetic coupling determines the final microstructures of the gel materials. It is challenging yet highly desired to develop robust hydrogels with a colloidal network structure by polymerization-induced phase separation.

Here, we report a series of poly(methacrylic acid) (PMAAc) hydrogels with a unique colloidal network structure developed by free-radical polymerization of methacrylic acid (MAAc) in the presence of *N*,*N*,*N*′,*N*′-tetramethylethylenediamine (TMEDA) that was usually used as the reaction accelerator. The structural evolution and underlying formation mechanism of colloidal hydrogels were revealed by a combination of dynamic light scattering measurements and optical microscopy. We found that hydrogen bond complexation between the carboxylic acid of reaction-produced PMAAc and the amine group of TMEDA at appropriate feeding concentrations led to the formation of primary colloidal particles that assembled into clusters and a colloidal network during the following polymerization process. The microstructure of the gels depended on the coupling of polymerization, hydrogen bond complexation, microphase separation, and gelation. These supramolecular hydrogels with a colloidal network exhibited robust mechanical properties, especially good stretchability. Such sponge-like gels were also applied for solar water evaporation and pollution absorption to produce clean water. We envision that this work can inspire the designing of other functional gels with controllable microstructures and properties through polymerization-induced phase separation.

EXPERIMENTAL SECTION

Materials. Methacrylic acid (MAAc), potassium persulfate (KPS), methacrylamide (MAAm), polyethyleneimine (PEI, 50% aqueous solution; molecular weight, 70 000), and triethylamine (TEA) were used as received from Aladdin Chemistry Co., Ltd. *N*,*N*,*N*′,*N*′-tetramethylethylenediamine (TMEDA) and ethylenediamine (EDA) were purchased from Sigma-Aldrich. The black carbon-based oily ink was obtained using a commercial Zebra marker. Millipore deionized water was used in all of the experiments.

Synthesis of Physical PMAAc Hydrogels. Physical PMAAc hydrogels were synthesized by free-radical polymerization of the aqueous precursor solution of MAAc in the presence of KPS as the initiator and TMEDA as the reaction accelerator. Certain amounts of MAAc and KPS (0.5 mol %, relative to MAAc) were dissolved in water. After degassing, a prescribed amount of TMEDA was added to the precursor solution. The obtained homogeneous solution was injected into a reaction cell consisting of a pair of glass substrates separated with a silicone spacer, which was subsequently kept in an oven at 70 °C for 6 h to complete the polymerization. The as-prepared hydrogels were then immersed in a large amount of water for one week to remove the residuals and reach the equilibrium state. The hydrogels were coded as PT-C_m-V_T, in which C_m and V_T are the feeding concentration of MAAc in M and the feeding volume fraction of TMEDA in vol % (relative to the precursor solution), respectively. Other physical hydrogels derived from the polymerization of MAAc in the presence of other amine/amide-containing molecules were prepared in a similar way by adding a certain amount of EDA, PEI, MAAm, or TEA to the precursor solution. All of the samples were prepared at a constant C_m of 1 M.

Characterization. UV−vis absorption spectra of the black carbon-based oily ink and dye solutions were obtained using an ultraviolet spectrophotometer (Shimadzu, UV 1800). Infrared spectra of TMEDA, PMAAc aqueous solution, and the PT-1-1 hydrogel were measured by attenuated total reflectance Fourier transform infrared spectroscopy (FTIR) (Nicolet iS10 ATR-FTIR; Thermo Scientific). All of the FTIR spectra were obtained at room temperature with 32 scans and a resolution of 4 cm^{-1} in the range of 4000−400 cm^{-1}. Size distributions of the aggregate particles formed at the initial stage of polymerization were measured by dynamic light scatting (DLS; Malvern Zetasizer Nano ZS). The precursor solution was sealed in a cuvette with 1 mm gap for DLS analysis at 70 °C. A digital microscope (Dino-Lite AM7515MT8A) was applied for in situ observation of the structural evolution during the polymerization process. The precursor solution was dripped between two glass slides with a spacer of ∼50 μm, which was then placed on a heating stage at 70 °C for in situ microscopy observation. Rheological behaviors of the hydrogels were measured using a DHR-2 rheometer (TA Instruments). To monitor the gel synthesis process, the precursor solution was directly transferred to the sample stage, with a spacing of 1 mm between the top 40 mm diameter parallel plate. Then, oscillatory shear was applied to the sample at 70 °C with a strain amplitude of 2% and a frequency of 1 Hz (in the linear region). Strain sweep from 1% to 230% was also performed on the hydrogel at 25 °C and a frequency of 1 Hz. The axial force was set as zero during the measurement. The composition of the equilibrated PT-1-1 hydrogel was measured by elemental analysis (EuroEA EA3000). The fraction of soluble species, φ_s, is calculated by the formula $\varphi_s = (m_0 - m_1)/m_0$, where m_0 and m_1 are the mass of the dried as-prepared gel and dried equilibrated gel, respectively, after swelling in water at room temperature for one week.

Microstructures of the hydrogels were observed with a field-emission scanning electron microscope (SEM; Hitachi S4800). The samples were prepared by freeze-drying and then cryogenically fractured in liquid nitrogen. The fractured cross section of the gel was coated with a thin layer of gold using a sputter coater. The accelerating voltage for SEM observation was 3 kV. In addition, microcomputed tomography (micro-CT; skysCan2211) was applied to characterize the microstructure of the hydrogel with a colloidal network in the hydrated state.

Mechanical properties of the hydrogels were measured on a commercial tensile tester (Instron 3343) at room temperature. For tensile tests, samples were cut from the hydrogel sheet into a dumbbell shape with an initial gauge length of 12 mm and a width of 2 mm. The stretch rate was 100 mm/min, and the nominal stress (σ) and strain (ε) were recorded. Young's modulus (E) of the gel was calculated from the initial slope of the tensile stress−strain curve with a strain below 10%. For compression tests, cylinder samples with a height of 9 mm and a diameter of 12.5 mm were prepared by polymerizing the precursor solutions in a syringe. The compression rate was 1 mm/min, and the nominal stress (σ') and strain (ε') were recorded.

To investigate the dye absorption capacity, the cylinder hydrogel of PT-1-1 (height of 9 mm and diameter of 12.5 mm) was subjected to a

https://doi.org/10.1021/acs.macromol.1c02129
Macromolecules XXXX, XXX, XXX−XXX

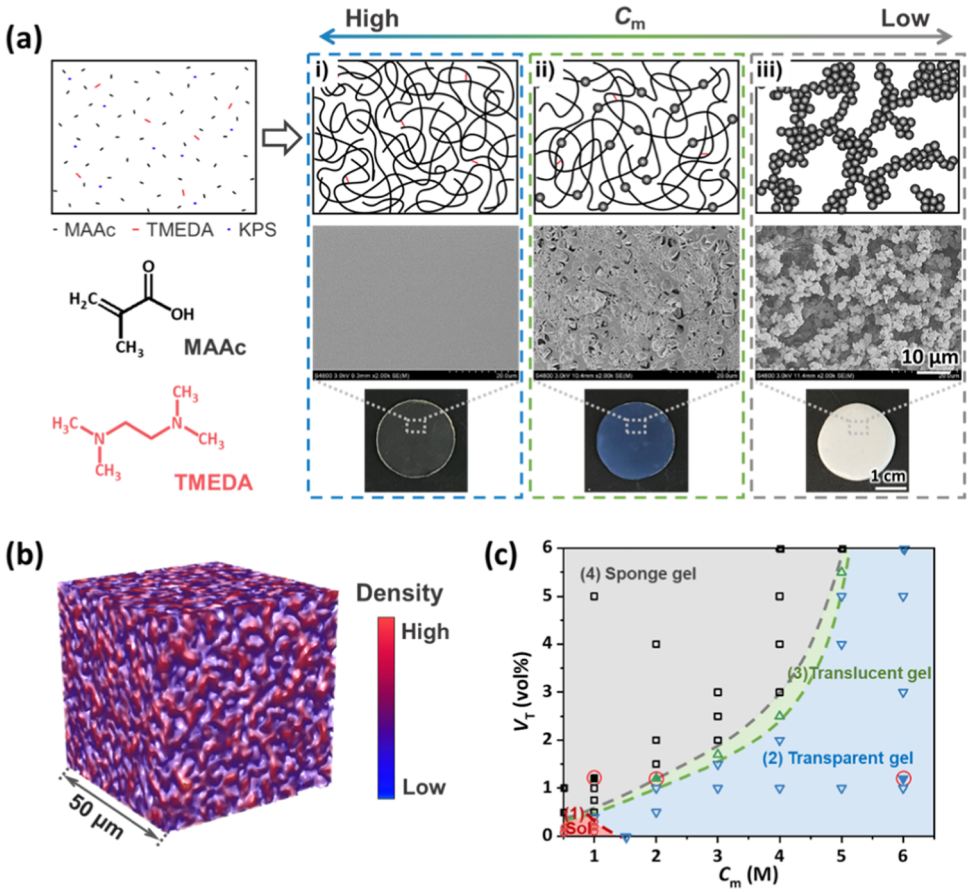

Figure 1. (a) Schematic for gel synthesis, the appearance, and SEM images of the hydrogels (PT-C_m-V_T) prepared with different feeding concentrations of MAAc (C_m) and TMEDA (V_T). (i) PT-1-1.2, (ii) PT-2-1.2, (iii) PT-6-1.2, as marked by red circles in panel (c). (b) Micro-CT morphology of the PT-1-1 gel in the hydrated state. Dimension: 50 × 50 × 50 μm^3. Color bar indicates different densities. (c) Diagram of the microstructures of the gels synthesized with different C_m and V_T. The samples are classified into four types based on their appearance and microstructure. Hollow symbols represent the experimental results.

compression force of 500 N to squeeze out the water, and then the gel was immediately placed in a 0.1 wt % neutral red dye solution. After the gel recovered its initial size, it was taken out and compressed to squeeze out the trapped solution. The concentrations of the dye in the original and squeezed solutions were measured by UV−vis spectroscopy. Water evaporation performance of the hydrogel was examined using a solar simulator (PLS−SXE300D; Beijing Perfect Light Technology) with solar irradiation density of 1 sun. Hydrogel sheets with a thickness of 2 mm were cut into quadrate pieces with an exposed area of 4 cm^2, which was placed atop the polystyrene (PS) foam floated on water in a glass beaker. The mass change of the water was recorded by a lab balance after a stabilization period under 1 sun irradiation for 30 min. During the evaporation process, the ambient temperature and the relative humidity were kept at 20 °C and 50%, respectively. The water loss originated from the surrounding blank PS foam under solar irradiation was subtracted from the total loss of water.

RESULTS AND DISCUSSION

Synthesis and Different Microstructures of Physical Gels. A series of physical hydrogels were synthesized via free-radical polymerization of MAAc in the presence of TMEDA. The obtained hydrogels were coded as PT-C_m-V_T, in which C_m and V_T are the feeding concentration of MAAc in M and feeding volume fraction of TMEDA in vol %, respectively. As shown in Figure 1a, the appearance of the hydrogels varied with the increase in C_m or with the decrease in V_T, from opaque to translucent and then to transparent, indicating the different microstructures of the gels. With the decrease in C_m (constant V_T: 1.2 vol %), the microstructure of the hydrogels changed from a uniform network to an irregular porous structure and then to a colloidal network composed of aggregates with diameters ranging from 1 to 2 μm, as revealed by SEM. The unique colloidal network structure of the gel in a hydrated state was confirmed by microcomputed tomography (micro-CT) (Figure 1b). The aggregates were connected to form a penetrating colloidal network, and the interspace was a continuous micron-sized channel and filled with water, suggesting that the freeze-drying process before SEM observation had little influence on the microstructure of the colloidal hydrogel. Therefore, in the following section, microstructures of the colloidal gels were characterized by SEM for simplicity.

The PMAAc hydrogels or viscous solutions prepared from precursor solutions with different C_m and V_T (in the range of 0.5−6 M and 0−6 vol %, respectively) can be divided into four regions according to the appearance and microstructure of the samples, as summarized in Figure 1c: (1) When both C_m and V_T were relatively low, viscous solutions rather than intact hydrogels were obtained due to the relatively low polymer content as well as insufficient entanglement and physical cross-linking. (2) When C_m was high yet V_T was relatively low; transparent gels with a uniform polymer network were formed by the increased polymer density and entanglements. (3) With

https://doi.org/10.1021/acs.macromol.1c02129
Macromolecules XXXX, XXX, XXX−XXX

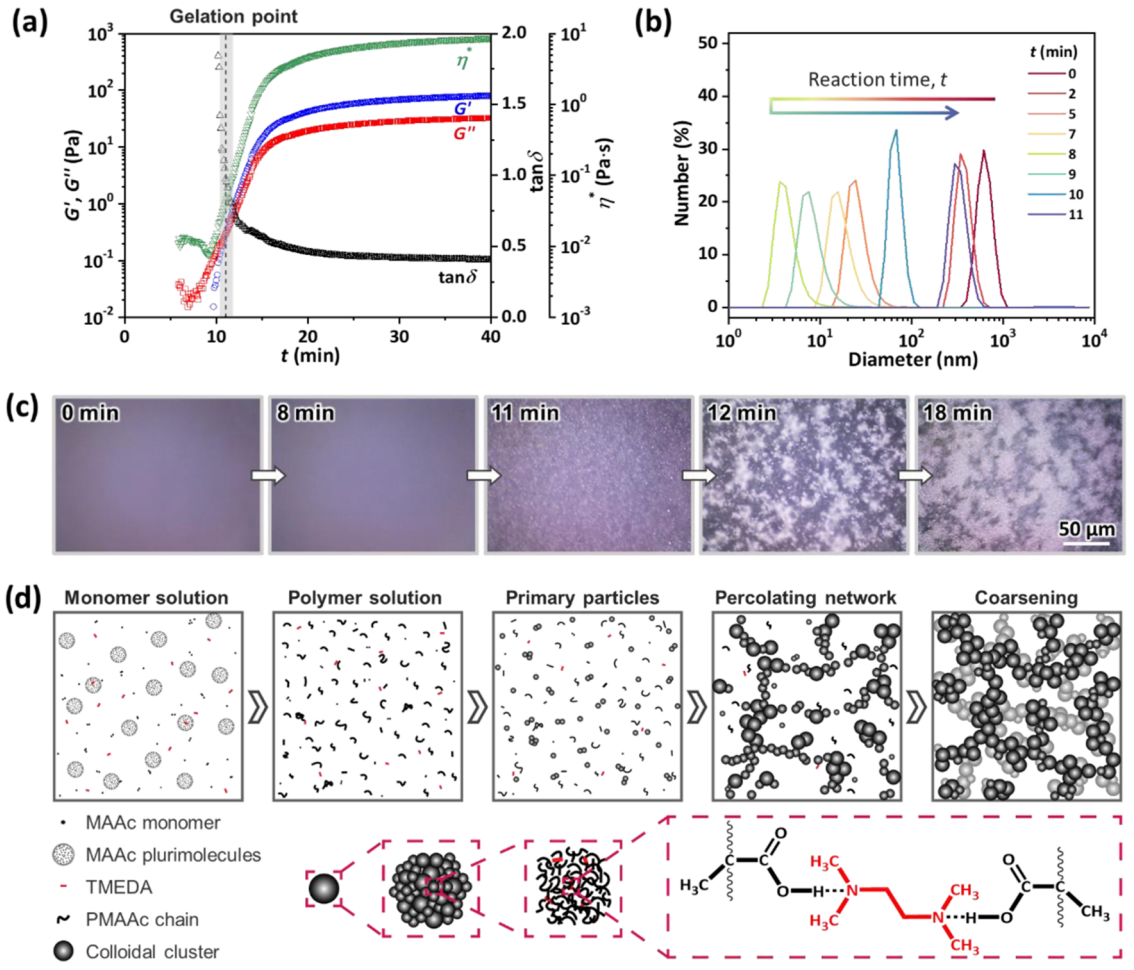

Figure 2. (a) Variations of storage modulus G', loss storage modulus G'', loss tangent tan δ, and complex viscosity η^* as a function of the reaction time t for the gel synthesis. (b, c) Dynamic light scatting (DLS) measurement (b) and in situ optical microscopy observation (c) during the synthesis of the PT-1-1 gel. (d) Illustration of the structural evolution during the synthesis of the colloidal hydrogel. The elements in the schematic are not in scale.

further increase in V_T on the basis of the above region, translucent gels with a porous structure were obtained, probably because of the microphase separation caused by the formation of hydrogen bond complexes between PMAAc and TMEDA. (4) When V_T continued to increase and C_m was relatively low, opaque hydrogels with a colloidal network were obtained due to the enhanced polymerization-induced phase separation. We should note that the critical V_T for phase separation varied nonlinearly with the increase in C_m. Relatively, a high V_T was required to retain the colloidal network structure in the hydrogel prepared with a higher C_m. This was because the enhanced entanglement at higher C_m should hinder the phase separation to some extent during the polymerization process.

According to the aforementioned results, there are two prerequisites for the polymerization-induced phase separation and formation of a colloidal network structure in hydrogels: (i) a certain amount of TMEDA to form hydrogen bond complexes with PMAAc that resulted in microphase separation and (ii) a relatively low C_m to favor the formation of colloidal particles rather than the entangled network between PMAAc chains.

Structural Evolution and Formation Mechanism of Colloidal Gels. It was remarkable to form the unique colloidal network structure in the physical hydrogels by direct polymerization of aqueous precursor solutions. There are two fundamental questions related to this phenomenon: (i) How does the microstructure form and develop during the polymerization of a precursor solution? (ii) What is the formation mechanism of this colloidal network structure? To address these problems, the PT-1-1 hydrogel system was selected to investigate the structural evolution during the gel synthesis and also to reveal the formation mechanism of the colloidal network.

Figure 2a showed the variation of rheological properties of the PT-1-1 system during the polymerization process. At the beginning of the reaction, the storage modulus, G', was lower than the loss modulus, G'', indicating the fluid-like behavior of the system. Then, G' and G'' formed a cross over, which was followed by a drastic increase in G' and G''. The gelation time was defined as the reaction time when $G' = G''$, corresponding to the formation of a percolating network. The gelation time for the PT-1-1 system was about 11 min. The relatively fast polymerization/gelation should be attributed to the presence of TMEDA, which usually acted as a reaction accelerator and decreased the reaction activation energy.[37] In addition, the complex viscosity of the system at the gelation point, η_g^*, was very low, ~0.04 Pa·s. For physical polymer gels, η_g^* was often in the range of 1−10 Pa·s due to the considerable entanglement between polymer chains when the gelation

https://doi.org/10.1021/acs.macromol.1c02129
Macromolecules XXXX, XXX, XXX−XXX

occurred,[32] which was larger than that (0.001−0.1 Pa·s) for physical gels with a colloidal network assembled from colloidal suspensions with a volume fraction of 0.02−0.3.[9,38,39] This result indicated that the appearance of a percolated network was induced by dynamical arrest of colloidal particles with the increased volume fraction during the polymerization.[40]

The formation of aggregate particles at the beginning of the polymerization was monitored by DLS (Figure 2b). Before the reaction started, MAAc monomers in the aqueous precursor solution formed plurimolecular aggregates with a diameter of several hundred nanometers due to the strong hydrogen bonding between the unionized MAAc units.[41−43] A typical Tyndall phenomenon of the MAAc solution without TMEDA also verified the presence of micron-sized droplets (Figure S1a). It should be noted that the subsequent polymerization process was rarely affected by the MAAc monomer aggregation.[42] In the absence of TMEDA, the reaction gradually consumed MAAc, accompanied by a gradual disappearance of the liquid−liquid phase separation interfaces. Consequently, the aggregate size gradually decreased from ∼600 to ∼1 nm, as the reaction time increased from 0 to 60 min (Figure S1b). This is probably because of the increased hydrophilicity of reaction-produced PMAAc chains with a hydrophobic backbone inside and carboxylic acid groups toward the aqueous environment, which facilitated their transfer from the small droplets to the surrounding continuous phase.[43−46] While in the presence of TMEDA, PMAAc polymer chains were produced by the reaction, which led to a decrease in the particle size, similar to the case without TMEDA (Figure 2b). However, the resulting PMAAc chains should be physically cross-linked by TMEDA molecules by forming hydrogen bonds between the carboxylic acid and amine groups. The hydrogen bond complexation resulted in decreased hydrophilicity of PMAAc chains, microphase separation, and the appearance of colloidal aggregates.[32] As the reaction continued, the size of the aggregated particles grew fast and reached a diameter about hundreds of nanometers in a few minutes (Figure 2b), which was different from the case without TMEDA.

Due to the detection limit of the DLS instrument, the growth of the aggregates after the gelation point was directly observed under a digital optical microscope. As shown in Figure 2c and Movie S1, the primary micron-sized colloidal particles were uniformly distributed in the suspension and moved rapidly during the polymerization process. The size of the particles continued to grow by capturing the free polymer chains or fusing with other particles. Then, large colloidal particles quickly aggregated into clusters with a diameter up to tens of micrometers during the collision and merging process. The mobility of the colloidal clusters decreased significantly with the growth in size, and a continuous network was formed as the large colloidal clusters became interconnected. With further proceeding of the reaction, the general morphology of the colloidal network did not change; instead, the colloidal network became coarsened by merging reaction-produced new colloids, finally resulting in sponge-like hydrogels consisting of colloidal particles.

The main driving force for polymerization-induced phase separation of PMAAc to form the colloidal network was the hydrogen bonding between the carboxylic acid group in PMAAc and the amine group in TMEDA.[47] The formation of hydrogen bonds was confirmed by FTIR. Compared to PMAAc solution, the peak of carbonyl stretching resonances of the PT-1-1 hydrogel shifted from 1698 to 1685 cm^{-1}, and a new peak appeared at 1548 cm^{-1} that is associated with the antisymmetric vibration of COO^- (Figure S2), indicating the formation of ionic hydrogen bonds between PMAAc and TMEDA.[48−50] Another evidence was the different appearance of PMAAc solution and MAAc solution after adding 1 vol % TMEDA. The white flocculent precipitate with a similar colloidal network structure was found in the former, while no precipitation was found in the latter (Figure S3). This result suggested that the aggregate particles were formed by hydrogen bond complexation between the reaction-produced PMAAc chain and the dopant molecule of TMEDA. We should note that the intra- and interchain hydrogen bonds, as well as the entanglements of PMAAc chains, also contributed to the robustness of the colloidal particles and the intact physical hydrogel.[51]

Based on these results, a possible formation mechanism of the colloidal network during the gel synthesis was proposed (Figure 2d). In the precursor solution, MAAc monomers formed nanosized plurimolecular aggregates, which were disrupted by polymerization of the monomers to produce PMAAc chains. The resulting PMAAc polymer chains formed hydrogen bond complexes with TMEDA, which reduced the hydrophilicity of PMAAc chains and resulted in microphase separation and formation of colloidal particles. The quantity and the size of colloidal particles increased as the polymerization continued and merged or connected to form larger clusters. The subsequent cluster crowding led to local dynamic arrest and the formation of the interconnected colloidal network. The colloidal network further coarsened through immobilizing newly formed free colloidal particles and polymer chains, in which the weaker colloidal particles and the trapped PMAAc chains served as an adhesive to produce an intact and robust physical hydrogel.

Influence of Temperature and Universality for Developing Colloidal Gels. The degree of microphase separation and the microstructure of resultant hydrogels depended on the density and strength of the hydrogen bonds between PMAAc and TMEDA, which were influenced by the composition and condition for gel synthesis. When the monomer concentration was fixed (C_m = 1 M), the TMEDA concentration, V_T, and the reaction temperature, T_R, should also affect the formation of hydrogen bond complexes and the microphase separation. The effects of V_T and T_R on the microstructure of the hydrogels are shown in Figure S4. As V_T or T_R decreased, the hydrogels gradually changed from a colloidal network to a micron-sized porous network decorated with some colloidal particles, which became smaller and finally disappeared. The decrease in V_T reduced the density of hydrogen bonds and suppressed the formation of particles and the colloidal network. The influence of T_R on the microphase separation was complicated because the decreased T_R not only enhanced the strength of hydrogen bonding but also weakened the hydrophobic interactions in the system. The weakened phase separation suggested that the hydrophobic interactions at an elevated temperature were also significant for the formation of the colloidal network.[52] The variations of V_T and T_R also influenced the polymerization kinetics. The coupling of the chemical reaction and microphase separation determined the microstructure of the hydrogels.

As aforementioned, the presence of TMEDA with multiple amine groups capable of forming hydrogen bonds with PMAAc chains was crucial for the reaction-induced phase separation

https://doi.org/10.1021/acs.macromol.1c02129
Macromolecules XXXX, XXX, XXX−XXX

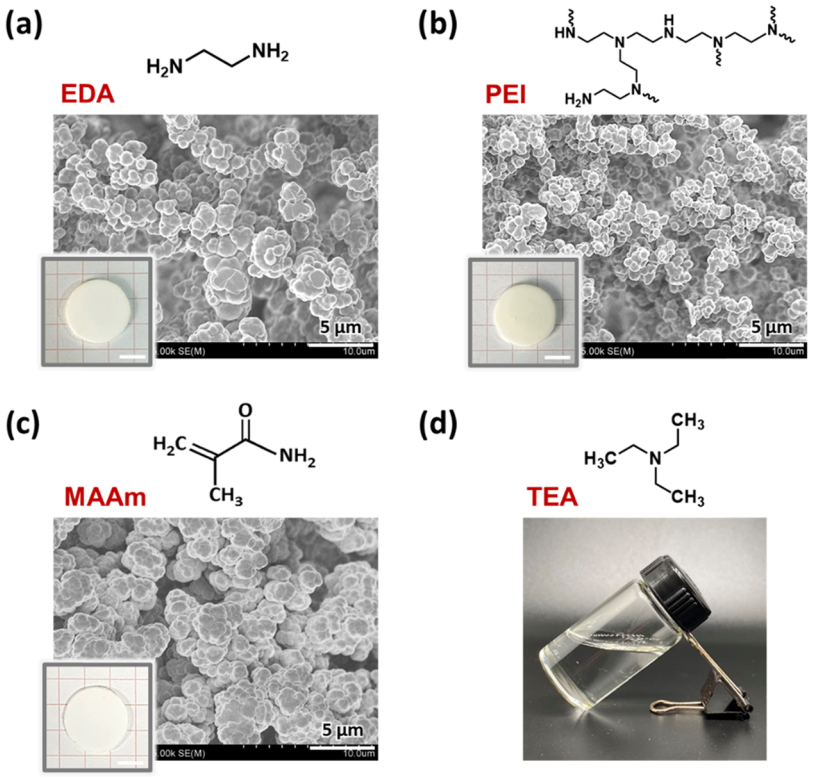

Figure 3. Microstructure of the colloidal hydrogels synthesized by polymerization of MAAc in the presence of (a) EDA, (b) PEI, or (c) copolymerization of MAAc and MAAm. Insets show the appearance of the gels. Scale bar: 1 cm. (d) Appearance of polymer solution synthesized by polymerization of MAAc in the presence of TEA. Chemical structures of the amine/amide-containing molecules are atop the SEM images.

and formation of the colloidal network. The universality of this mechanism for developing colloidal hydrogels was examined using other small molecules containing multiple amine groups. For example, when ethylenediamine (EDA) or polyethyleneimine (PEI) was added to the precursor solution of MAAc, opaque hydrogels with a similar colloidal network were obtained due to the strong hydrogen bonding interaction between EDA/PEI and PMAAc chains (Figure 3a,b). Hydrogels with a colloidal network can also be prepared by introducing amide-containing monomers for copolymerization with MAAc. As shown in Figure 3c, the poly(methacrylamide-*co*-methacrylic acid) [P(MAAm-*co*-MAAc)] hydrogel had a typical colloidal network because strong intra- and interchain hydrogen bonds were formed between randomly distributed amide and carboxylic acid groups of the copolymers that facilitated microphase separation.[32] However, phase separation was absent during the gel synthesis of the PMAAc hydrogel in the presence of small monoamines such as triethylamine (TEA) because it cannot form multiple hydrogen bonds to physically cross-link the PMAAc chains (Figure 3d). Although hydrogen bond complexes were demonstrated in this work, we believe that other noncovalent bonds such as ionic bonds and coordination bonds could also be used for the polymerization-induced microphase separation and formation of the colloidal network.[53]

Mechanical Properties of the Colloidal Hydrogel. Different from the common physical gels with the colloidal network structure,[2,9,32,54] our PMAAc hydrogels with a colloidal network were stable after swelling in water. After incubating the as-prepared gel in water for one week to reach the equilibrium state, the colloidal hydrogel PT-1-1 rarely changed its dimensions. The antiswelling property was attributed to the robust hydrogen bonds between PMAAc and TMEDA that served as physical cross-links of the gel matrix.[55] As expected, TMEDA molecules were well retained in the colloidal hydrogel, as confirmed by the elemental analysis result (Table S1). The total fraction of soluble species was 6.5 wt %, which was examined by measuring the solid content of the gel before and after the swelling process. It can be estimated that about 1.8 wt % of TMEDA and 6.6 wt % of MAAc relative to the respective content in the precursor solution were diffused out of the gel during the swelling process, thus the soluble species should consist of a small proportion of unbound TMEDA and a large proportion of unreacted MAAc monomers and mobile PMAAc chains in the colloidal gel. The colloidal hydrogels (e.g., PT-1-1 gel) also possessed moderate mechanical properties, which were examined by tensile and compression tests. As shown in Figure 4a, the PT-1-1 hydrogel was soft and stretchable, with a tensile breaking strain of 525%, breaking stress of 22.1 kPa, and Young's modulus of 4.4 kPa. We should note that the content of TMEDA was very low, ~6 mol % relative to the MAAc unit; C_m was 1 M in this work, much lower than that for the synthesis of tough hydrogels with dense hydrogen bonds.[20,23,56] Although the mechanical properties of the colloidal hydrogel were not as excellent as other tough hydrogels,[19−24,56−58] they were much better than the most existing colloidal hydrogels usually having weak interactions between the particles.[8−15] Beyond the notable stretchability, the colloidal hydrogel also showed the good self-recovery property at room temperature (Figure S5). During the cyclic tensile test of the gel with a maximum strain of 300%, the residual strain decreased rapidly after unloading and finally disappeared after waiting for 5 min, and the hysteresis ratio

https://doi.org/10.1021/acs.macromol.1c02129
Macromolecules XXXX, XXX, XXX−XXX

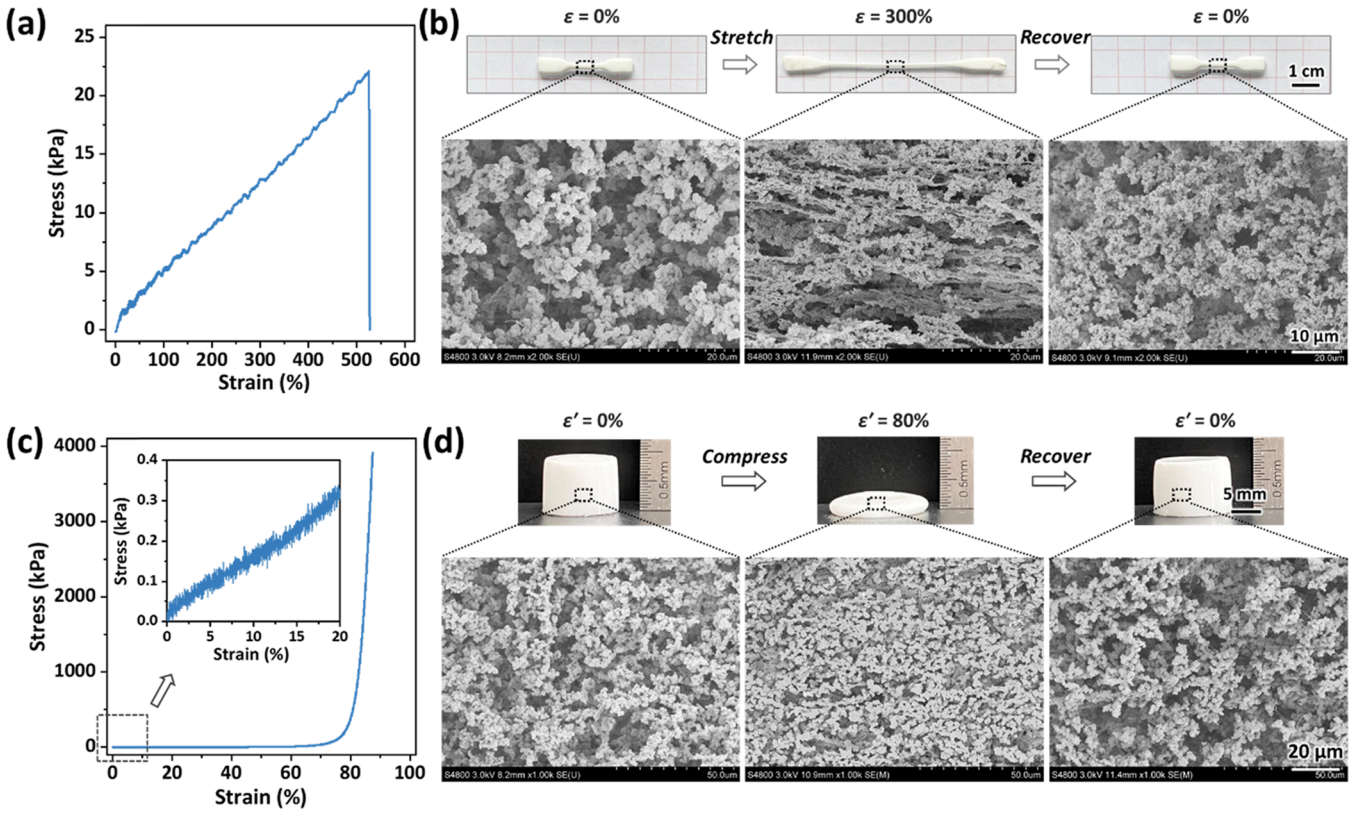

Figure 4. (a) Tensile stress−strain curve of the PT-1-1 hydrogel. (b) Appearances and microstructures of the PT-1-1 hydrogel in the original state, after being stretched to a strain of 300% and recovered after unloading for 5 min. (c) Compression stress−strain curve of the PT-1-1 hydrogel. (d) Appearances and microstructures of the PT-1-1 hydrogel in the original state, after being compressed to a strain of 80% and recovered after unloading for 30 min.

reached above 80% after waiting for 15 min. The incomplete recovery indicated that the colloidal network was partially destroyed during stretching. The microstructure of the hydrogel at different stages of tensile loading and unloading was investigated by SEM. As shown in Figure 4b, the colloidal network was highly deformed when the gel experienced a tensile strain of 300%, upon which large colloidal clusters were dissociated into small particles. Remarkably, the colloidal particles and clusters were connected by stretchable fibers like a necklace. After unloading, the stretched fibers reverted to colloidal particles, and the microstructure of the gel recovered the colloidal network. However, the colloidal particles/clusters of the hydrogel became more uniform after the unloading and recovery process. This finding was consistent with the result of self-recovery of the gel (i.e., no residual strain but not full recovery). The excellent elasticity of the hydrogel should be related to the robustness of the colloidal particles joined with the adhesive PMAAc chains. The relatively weak particles can be highly deformed into a fiber-like shape upon loading and capable of recovering the particulate shape after unloading. The structural evolution of the colloidal network at different tensile strains was also correlated to the rheological result of the hydrogel by the strain-sweep measurement. As shown in Figure S6, a weak shear thinning was observed in the colloidal gel when subjected to a small shear strain (γ < 50%), which resulted in rearrangement of the colloidal clusters,[54] while at a larger shear strain (γ > 50%), a sharp increase in the storage modulus was observed, indicating the strain-induced dissociation and fibrosis of the colloidal clusters within the gel.

The colloidal hydrogel also showed good performance under compression. As shown in Figure 4c, the hydrogel did not fracture even under the largest applied force (500 N) of the tensile tester, with the compression strain (ε') of 88% and the compression stress of 3.9 MPa. The hydrogel also had good self-recovery ability after unloading, as demonstrated by cyclic compression tests. At a maximum ε' of 80%, the cylinder hydrogel can fully recover its original height after unloading and being immersed in water for 30 min (Figure S7a). The variations of the microstructures of the gel during the compression and recovery process are shown in Figure 4d. The porous colloidal network became compact after the compression and restored the initial structure after unloading, indicating the good elasticity of the colloidal gel. The resilience of the hydrogel was examined by cyclic compressive loading and unloading (Figure S7b,c). The result showed that the gel can fully recover its size, yet the maximum compression stress decreased to some extent, probably because of the structural adjustment and partial destruction of the colloidal network. We noticed a sharp increase in the compressive stress when ε' exceeded 80%, suggesting the disappearance of the cavity and the densification of the colloidal network under compression. As shown in Figure S8, the cross section of the colloidal gel at ε' of 88% was compact and uniform with a few visible pores. During the compression process, the water inside the hydrogel was readily squeezed out. When the equilibrated PT-1-1 gel was subjected to a compressing force of 500 N, the water content (q) decreased from 90.3 to 8.6 wt %, indicating that 90.5% of the water was expelled out of the gel. This result suggested that most water in the colloidal gel was capillary

https://doi.org/10.1021/acs.macromol.1c02129
Macromolecules XXXX, XXX, XXX−XXX

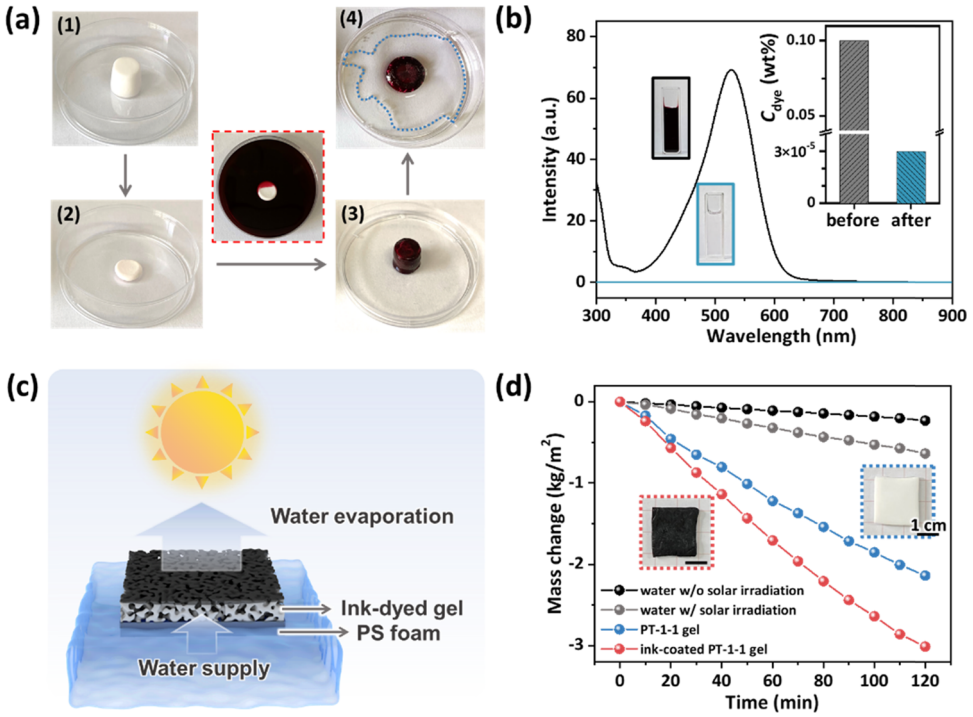

Figure 5. (a) Removing of dye molecules using the colloidal gel. The PT-1-1 gel was compressed to squeeze out the water and then placed in the solution of a neutral red dye to absorb the dye solution. After compression, clean water was squeezed out of the gel. (b) UV−vis spectra of the original dye solution and the squeezed solution after gel absorption. (c) Schematic for the hydrogel-based solar vapor generator (SVG). (d) Mass change of different solar vapor generators during simulated solar irradiation at room temperature and relative humidity of 50%.

trapped in the micropores, which can be readily discharged by compression and spontaneously reabsorbed after unloading, just like a sponge.

Colloidal Gels for Dye Adsorption and Solar Vapor Generation. The colloidal hydrogels with a unique porous structure and robust mechanical properties should find applications in molecular adsorption, particle separation, tissue engineering, solar harvesting, etc.[59−62] In the following, two examples are designed to show the applications of the colloidal hydrogels in the removal of dye molecules and the generation of solar steam. The porous structure afforded the colloidal gel with a high surface area to volume ratio, favoring high-efficiency dye adsorption and removing from aqueous solutions. As shown in Figure 5a, the PT-1-1 gel was compressed to a strain of 88% to squeeze out the water. The resultant gel sponge was immersed into an aqueous solution with 0.1 wt % neutral red dye, in which the gel recovered its initial size by absorbing the dye solution. After waiting for a while, colorless water was squeezed out of the gel matrix by compression, while the dye molecules with amine groups were absorbed by the gel by forming hydrogen bonds with the carboxyl groups of PMAAc chains.[63] The efficiency was assessed by the variation of the concentration of dye molecules before and after the adsorption/removing process. According to the absorption spectra of the original solution and the purified water in Figure 5b, the concentration of dye molecules decreased from 1×10^{-1} to 3×10^{-5} wt %, indicating the high efficiency of the colloidal gel to remove dye molecules for water purification.

The colloidal gel was also devised into a solar vapor generator (SVG) (Figure 5c), which is useful for seawater desalination and clean water generation. The unique porous structure of the colloidal gel with micron-sized channels should facilitate the rapid transportation of water.[25,64] The upper surface of the PT-1-1 gel was dyed with black ink to improve the light-to-heat conversion efficiency (Figure S9); the gel was placed atop a polystyrene (PS) foam as the floating support. When exposed to simulated solar irradiation of 1 sun (1 kW m^{-2}), the local temperature of the hydrogel surface was measured by an infrared radiation camera (Figure S10). For the SVG with the ink-dyed PT-1-1 gel, the local temperature increased from 20 to 34 °C within 5 min of solar irradiation and then reached an equilibrium value of ∼40 °C. In contrast, the surface temperature of the blank PT-1-1 gel and the blank PS foam increased slowly and finally stabilized at ∼30 °C. The SVG could generate vapor with a steady evaporation rate during the test time period. The averaged evaporation rate of the SVGs with and without ink was 1.50 and 1.07 kg m^{-2} h^{-1}, respectively, much higher than that of common water evaporation (0.32 kg m^{-2} h^{-1}) under the same condition (Figure 5d). The evaporation energy conversion efficiency of the SVG, η, was calculated by $\eta = \dot{m}h_e/P_{in}$, where $\dot{m}$ is the mass flux, h_e is the equivalent evaporation enthalpy, and P_{in} is the solar irradiation power (see details in Figure S11).[64,65] As shown in Figure S12, η of the SVG without ink was 64.6%, which increased to 91.0% after dyed with the ink, comparable to the most existing hydrogel-based SVGs.[25,66−70]

CONCLUSIONS

In summary, we have developed a series of sponge-like physical hydrogels with a unique colloidal network by polymerization-induced microphase separation, in which the reaction-produced PMAAc chains formed compact hydrogen bond complexes with the small molecules bearing multiple amine groups. The microstructures of the hydrogels depended on the coupling of polymerization, phase separation, and gelation

https://doi.org/10.1021/acs.macromol.1c02129
Macromolecules XXXX, XXX, XXX−XXX

processes, which were influenced by C_m, V_T, and T_R. Colloidal hydrogels were formed at a relatively low C_m in the presence of a certain amount of TMEDA, which facilitated the phase separation and the formation of colloidal particles and clusters that finally combined to form a continuous colloidal network during the polymerization/gelation process. These physical colloidal hydrogels were stable in water and possessed robust mechanical properties, especially good stretchability. It was revealed that colloidal aggregates were reversibly deformed into a fiber-like shape upon stretching and recovered the particulate shape after unloading. Such features endowed the gel with good self-recovery ability. These colloidal hydrogels were further applied to remove dye molecules and generate solar vapor to produce clean water. The strategy to develop robust colloidal hydrogels by polymerization-induced phase separation could be extended to other systems with strong associative interactions. It should be an interesting research subject to engineer the microstructures and macroscopic properties of functional materials by tailoring the phase separation during the reaction process.

■ ASSOCIATED CONTENT

Supporting Information

The Supporting Information is available free of charge at https://pubs.acs.org/doi/10.1021/acs.macromol.1c02129.

Additional experimental results, including FTIR spectra, UV−vis spectra, DLS result, elemental analysis result, SEM images, strain-sweep spectra, stress−strain curves, and water evaporation performance (PDF)

In situ observation of structural evolution during the synthesis of the colloidal hydrogel (PT-1-1) with an optical microscope. The recording is started after the appearance of micron-sized particles (i.e. the reaction time of ∼11 min) (Movie S1) (MP4)

■ AUTHOR INFORMATION

Corresponding Author

Zi Liang Wu − *Ministry of Education Key Laboratory of Macromolecular Synthesis and Functionalization, Department of Polymer Science and Engineering, Zhejiang University, Hangzhou 310027, China;* orcid.org/0000-0002-1824-9563; Email: wuziliang@zju.edu.cn

Authors

Xin Ning Zhang − *Ministry of Education Key Laboratory of Macromolecular Synthesis and Functionalization, Department of Polymer Science and Engineering, Zhejiang University, Hangzhou 310027, China;* orcid.org/0000-0002-3617-143X

Cong Du − *Ministry of Education Key Laboratory of Macromolecular Synthesis and Functionalization, Department of Polymer Science and Engineering, Zhejiang University, Hangzhou 310027, China*

Zhou Wei − *Hangzhou Toka Ink Co., Ltd., Hangzhou 310018, China*

Miao Du − *Ministry of Education Key Laboratory of Macromolecular Synthesis and Functionalization, Department of Polymer Science and Engineering, Zhejiang University, Hangzhou 310027, China;* orcid.org/0000-0003-0095-9089

Qiang Zheng − *Ministry of Education Key Laboratory of Macromolecular Synthesis and Functionalization, Department of Polymer Science and Engineering, Zhejiang University, Hangzhou 310027, China*

Complete contact information is available at: https://pubs.acs.org/10.1021/acs.macromol.1c02129

Notes

The authors declare no competing financial interest.

■ ACKNOWLEDGMENTS

This research was supported by the National Natural Science Foundation of China (51973189, 51773179) and Natural Science Foundation of Zhejiang Province of China (LR19E030002).

■ REFERENCES

(1) Mezzenga, R.; Schurtenberger, P.; Burbidge, A.; Michel, M. Understanding foods as soft materials. *Nat. Mater.* **2005**, *4*, 729−740.

(2) Stradner, A.; Romer, S.; Urban, C.; Schurtenberger, P. Aggregation and gel formation in biopolymer solutions. *Progr. Colloid. Polym. Sci.* **2001**, *118*, 136−140.

(3) Dickinson, E. Colloids in food: ingredients, structure, and stability. *Annu. Rev. Food Sci. Technol.* **2015**, *6*, 211−233.

(4) Gentile, L. Protein−polysaccharide interactions and aggregates in food formulations. *Curr. Opin. Colloid Interface Sci.* **2020**, *48*, 18−27.

(5) Fang, Y.; Han, E.; Zhang, X-X.; Jiang, Y.; Lin, Y.; Shi, J.; Wu, J.; Meng, L.; Gao, X.; Griffin, P. J.; Xiao, X.; Tsai, H-M.; Zhou, H.; Zuo, X.; Zhang, Q.; Chu, M.; Zhang, Q.; Gao, Y.; Roth, L. K.; Bleher, R.; Ma, Z.; Jiang, Z.; Yue, J.; Kao, C-M.; Chen, C-T.; Tokmakoff, A.; Wang, J.; Jaeger, H. M.; Tian, B. Dynamic and programmable cellular-scale granules enable tissue-like materials. *Matter* **2020**, *2*, 948−964.

(6) Zhang, Y.; Gao, W.; Chen, Y.; Escajadillo, T.; Ungerleider, J.; Fang, R. H.; Christman, K.; Nizet, V.; Zhang, L. Self−assembled colloidal gel using cell membrane−coated nanosponges as building blocks. *ACS Nano* **2017**, *11*, 11923−11930.

(7) Shaw, S.; Yuan, B.; Tian, X.; Miller, K. J.; Cote, B. M.; Colaux, J. L.; Migliori, A.; Panthani, M. G.; Cademartiri, L. Building materials from colloidal nanocrystal arrays: preventing crack formation during ligand removal by controlling structure and solvation. *Adv. Mater.* **2016**, *28*, 8892−8899.

(8) Lin, M. Y.; Lindsay, H. M.; Weitz, D. A.; Ball, R. C.; Klein, R.; Meakin, P. Universality in colloid aggregation. *Nature* **1989**, *339*, 360−362.

(9) Tsurusawa, H.; Leocmach, M.; Russo, J.; Tanaka, H. Direct link between mechanical stability in gels and percolation of isostatic particles. *Sci. Adv.* **2019**, *5*, No. eaav6090.

(10) Patrick Royall, C. P.; Williams, S. R.; Ohtsuka, T.; Tanaka, H. Direct observation of a local structural mechanism for dynamic arrest. *Nat. Mater.* **2008**, *7*, 556−561.

(11) Piazza, R.; Pietro, G. Di. Phase separation and gel−like structures in mixtures of colloids and surfactant. *Europhys. Lett.* **1994**, *28*, 445−450.

(12) Manley, S.; Wyss, H. M.; Miyazaki, K.; Conrad, J. C.; Trappe, V.; Kaufman, L. J.; Reichman, D. R.; Weitz, D. A. Glasslike arrest in spinodal decomposition as a route to colloidal gelation. *Phys. Rev. Lett.* **2005**, *95*, No. 238302.

(13) Segrè, P.; Prasad, V.; Schofield, A.; Weitz, D. A. Glasslike kinetic arrest at the colloidal-gelation transition. *Phys. Rev. Lett.* **2001**, *86*, 6042−6045.

(14) Trappe, V.; Sandkühler, P. Colloidal gels: low−density disordered solid−like states. *Curr. Opin. Colloid Interface Sci.* **2004**, *8*, 494−500.

(15) Tanaka, H.; Araki, T. Spontaneous coarsening of a colloidal network driven by self−generated mechanical stress. *Europhys. Lett.* **2007**, *79*, 58003.

(16) Anderson, V. J.; Lekkerkerker, H. W. Insights into phase transition kinetics from colloid science. *Nature* **2002**, *416*, 811−815.

(17) Lu, P. J.; Zaccarelli, E.; Ciulla, F.; Schofield, A. B.; Sciortino, F.; Weitz, D. A. Gelation of particles with short-range attraction. *Nature* **2008**, *453*, 499−503.
(18) Whitesides, G. M.; Grzybowski, B. Self-assembly at all scales. *Science* **2002**, *295*, 2418−2421.
(19) Creton, C. 50th Anniversary perspective: networks and gels: soft but dynamic and tough. *Macromolecules* **2017**, *50*, 8297−8316.
(20) Hu, X.; Vatankhah-Varnoosfaderani, M.; Zhou, J.; Li, Q.; Sheiko, S. S. Weak hydrogen bonding enables hard, strong, tough, and elastic hydrogels. *Adv. Mater.* **2015**, *27*, 6899−6905.
(21) Yu, H. C.; Zheng, S. Y.; Fang, L.; Ying, Z.; Du, M.; Wang, J.; Ren, K.; Wu, Z. L.; Zheng, Q. Reversibly transforming a highly swollen polyelectrolyte hydrogel to an extremely tough one and its application as a tubular grasper. *Adv. Mater.* **2020**, *32*, No. 2005171.
(22) Yuan, T.; Cui, X.; Liu, X.; Qu, X.; Sun, J. Highly tough, stretchable, self−healing and recyclable hydrogels reinforced by in situ−formed polyelectrolyte complex nanoparticles. *Macromolecules* **2019**, *52*, 3141−3149.
(23) Zhang, X. N.; Wang, Y. J.; Sun, S.; Hou, L.; Wu, P.; Wu, Z. L.; Zheng, Q. A tough and stiff hydrogel with tunable water content and mechanical properties based on the synergistic effect of hydrogen bonding and hydrophobic interaction. *Macromolecules* **2018**, *51*, 8136−8146.
(24) Du, C.; Zhang, X. N.; Sun, T. L.; Du, M.; Zheng, Q.; Wu, Z. L. Hydrogen−bond association−mediated dynamics and viscoelastic properties of tough supramolecular hydrogels. *Macromolecules* **2021**, *54*, 4313−4325.
(25) Zhu, F.; Wang, L.; Demir, B.; An, M.; Wu, Z. L.; Yin, J.; Xiao, R.; Zheng, Q.; Qian, J. Accelerating solar desalination in brine through ion activated hierarchically porous polyion complex hydrogels. *Mater. Horiz.* **2020**, *7*, 3187−3195.
(26) Zhu, C. N.; Zheng, S. Y.; Qiu, H. N.; Du, C.; Du, M.; Wu, Z. L.; Zheng, Q. Plastic−like supramolecular hydrogels with polyelectrolyte/surfactant complexes as physical cross−links. *Macromolecules* **2021**, *54*, 8052−8066.
(27) Kim, S.; Huang, J.; Lee, Y.; Dutta, S.; Yoo, H. Y.; Jung, Y. M.; Jho, Y.; Zeng, H.; Hwang, S. Complexation and coacervation of like−charged polyelectrolytes inspired by mussels. *Proc. Natl. Acad. Sci. U.S.A.* **2016**, *113*, E847−E853.
(28) Dong, Z.; Cui, H.; Zhang, H.; Wang, F.; Zhan, X.; Mayer, F.; Nestler, B.; Wegener, M.; Levkin, P. A. 3D printing of inherently nanoporous polymers via polymerization−induced phase separation. *Nat. Commun.* **2021**, *12*, No. 247.
(29) Mredha, M. T. I.; Pathak, S. K.; Tran, V. T.; Cui, J.; Jeon, I. Hydrogels with superior mechanical properties from the synergistic effect in hydrophobic−hydrophilic copolymers. *Chem. Eng. J.* **2019**, *362*, 325−338.
(30) Lu, H.; Xing, Z.; Chen, M.; Yu, K.; Fu, Y. Q. Solvent−aided phase separation in hydrogel towards significantly enhanced mechanoresponsive strength. *Acta Mech. Sin.* **2021**, *37*, 757−766.
(31) Li, X.; Cui, K.; Sun, T. L.; Meng, L.; Yu, C.; Li, L.; Creton, C.; Kurokawa, T.; Gong, J. P. Mesoscale bicontinuous networks in self−healing hydrogels delay fatigue fracture. *Proc. Natl. Acad. Sci. U.S.A.* **2020**, *117*, 7606−7612.
(32) Zhang, X. N.; Du, C.; Du, M.; Zheng, Q.; Wu, Z. L. Kinetic insights into glassy hydrogels with hydrogen bond complexes as the cross−links. *Mater. Today Phys.* **2020**, *15*, No. 100230.
(33) Lee, J. C. Polymerization-induced phase separation. *Phys. Rev. E* **1999**, *60*, 1930−1935.
(34) Chirila, T. V.; Chen, Y. C.; Griffin, B. J.; Constable, I. J. Hydrophilic sponges based on 2−hydroxyethyl methacrylate. I. effect of monomer mixture composition on the pore size. *Polym. Int.* **1993**, *32*, 221−232.
(35) Donthula, S.; Mandal, C.; Schisler, J.; Leventis, T.; Meador, M. A. B.; Sotiriou−Leventis, C.; Leventis, N. Nanostructure−dependent marcus−type correlation of the shape recovery rate and the Young's modulus in shape memory polymer aerogels. *ACS Appl. Mater. Interfaces* **2018**, *10*, 23321−23334.
(36) Leventis, N.; Sotiriou-Leventis, C.; Chandrasekaran, N.; Mulik, S.; Larimore, Z. J.; Lu, H.; Churu, G.; Mang, J. T. Multifunctional polyurea aerogels from isocyanates and water. a structure−property case study. *Chem. Mater.* **2010**, *22*, 6692−6710.
(37) Feng, X. D.; Guo, X. Q.; Qiu, K. Y. Study of the initiation mechanism of the vinyl polymerization with the system persulfate/*N*,*N*,*N*′,*N*′−tetramethylethylenediamine. *Makromol. Chem.* **1988**, *189*, 77−83.
(38) Bode, F.; Silva, M. A.; Drake, A. F.; Ross-Murphy, S. B.; Dreiss, C. A. Enzymatically cross-linked tilapia gelatin hydrogels: physical, chemical, and hybrid networks. *Biomacromolecules* **2011**, *12*, 3741−3752.
(39) Gwon, S. H.; Yoon, J.; Seok, H. K.; Oh, K. H.; Sun, J-Y. Gelation dynamics of ionically crosslinked alginate gel with various cations. *Macromol. Res.* **2015**, *23*, 1112−1116.
(40) Trappe, V.; Prasad, V.; Cipelletti, L.; Segre, P. N.; Weitz, D. A. Jamming phase diagram for attractive particles. *Nature* **2001**, *411*, 772−775.
(41) Rajan, C. R.; Srinivas, Y. S.; Ponrathnam, S.; Radhakrishnan, K.; Nayak, U. V. Hydrophobic effects in the copolymerization of methacrylic acid with acrylamide. *J. Polym. Sci., Part C: Polym. Lett.* **1987**, *25*, 73−77.
(42) Chapiro, A. Polymerization and copolymerization in associated monomer aggregates. *Eur. Polym. J.* **1973**, *9*, 417−427.
(43) Lei, Z.; Wu, B.; Wu, P. Hierarchical network-augmented hydroglasses for broadband light management. *Research* **2021**, *2021*, No. 4515164.
(44) Ponrathnam, S.; Rao, S. P.; Kapur, S. L. Collapsed conformation of poly(methacrylic acid) chain containing nonionic hydrophilic units. *J. Polym. Sci.: Polym. Chem. Ed.* **1978**, *16*, 2183−2190.
(45) Kogej, K. Thermodynamic analysis of the conformational transition in aqueous solutions of isotactic and atactic poly(methacrylic acid) and the hydrophobic effect. *Polymers* **2016**, *8*, 168.
(46) Sedlák, M.; Konak, C.; Dybal, J. Heat−set poly(ethylacrylic acid) nanoparticles: combined light scattering, calorimetric, and FTIR Study. *Macromolecules* **2009**, *42*, 7439−7446.
(47) Meot-Ner Mautner, M. The ionic hydrogen bond. *Chem. Rev.* **2005**, *105*, 213−284.
(48) Zhang, H. J.; Sun, T. L.; Zhang, A. K.; Ikura, Y.; Nakajima, T.; Nonoyama, T.; Kurokawa, T.; Ito, O.; Ishitobi, H.; Gong, J. P. Tough physical double−network hydrogels based on amphiphilic triblock copolymers. *Adv. Mater.* **2016**, *28*, 4884−4890.
(49) Bayramgil, N. P. Thermal degradation of [poly(N−vinylimidazole)−polyacrylic acid] interpolymer complexes. *Polym. Degrad. Stab.* **2008**, *93*, 1504−1509.
(50) Li, C. Y.; Zheng, S. Y.; Du, C.; Ling, J.; Zhu, C. N.; Wang, Y. J.; Wu, Z. L.; Zheng, Q. Carbon dot/poly (methylacrylic acid) nanocomposite hydrogels with high toughness and strong fluorescence. *ACS Appl. Polym. Mater.* **2020**, *2*, 1043−1052.
(51) Robin, C.; Lorthioir, C.; Amiel, C.; Fall, A.; Ovarlez, G.; Le Coeur, C. Unexpected rheological behavior of concentrated poly(methacrylic acid) aqueous solutions. *Macromolecules* **2017**, *50*, 700−710.
(52) Sedlák, M. Homopolymer self−assembly into stable nanoparticles: concerted action of hydrophobic association and hydrogen bonding in thermoresponsive poly(alkylacrylic acid)s. *J. Phys. Chem. B* **2012**, *116*, 2356−2364.
(53) Luo, F.; Sun, T. L.; Nakajima, T.; Kurokawa, T.; Li, X.; Guo, H.; Huang, Y.; Zhang, H.; Gong, J. P. Tough polyion-complex hydrogels from soft to stiff controlled by monomer structure. *Polymer* **2017**, *116*, 487−497.
(54) Chan, H. K.; Mohraz, A. Two−step yielding and directional strain−induced strengthening in dilute colloidal gels. *Phys. Rev. E* **2012**, *85*, No. 041403.
(55) Zou, Q.; Zhu, Y.; Ruan, Y.; Zhang, R.; Liu, G. Coarse-grained soft-clusters remain non-diffusing in the melt state. *Giant* **2021**, *8*, No. 100070.

https://doi.org/10.1021/acs.macromol.1c02129
Macromolecules XXXX, XXX, XXX−XXX

(56) Wang, Y. J.; Zhang, X. N.; Song, Y.; Zhao, Y.; Chen, L.; Su, F.; Li, L.; Wu, Z. L.; Zheng, Q. Ultrastiff and tough supramolecular hydrogels with a dense and robust hydrogen bond network. *Chem. Mater.* **2019**, *31*, 1430−1440.
(57) Zhu, C. N.; Bai, T.; Wang, H.; Ling, J.; Huang, F.; Hong, W.; Zheng, Q.; Wu, Z. L. Dual-encryption in a shape-memory hydrogel with tunable fluorescence and reconfigurable architecture. *Adv. Mater.* **2021**, *33*, No. 2102023.
(58) Lian, W. Z.; Fan, Z. W.; Cui, K.; Yin, P.; Yang, J.; Jiang, H.; Tang, L.; Sun, T. Tough hydrogels with dynamic H-bonds: Structural heterogeneities and mechanical performances. *Macromolecules* **2021**, *54*, 8996−9006.
(59) Ayral, A.; Guizard, C.; Cot, L. Synthesis and application of hybrid organic−inorganic colloidal gels. *J. Mater. Sci. Lett.* **1994**, *13*, 1538−1539.
(60) Kerch, H. M.; et al. Characterization of porosity over many length scales: application to colloidal gels. *J. Mater. Res.* **1999**, *14*, 1444−1454.
(61) Wang, Q.; Wang, L.; Detamore, M. S.; Berkland, C. Biodegradable colloidal gels as moldable tissue engineering scaffolds. *Adv. Mater.* **2008**, *20*, 236−239.
(62) Gu, J.; Zhao, Y.; Guan, Y.; Zhang, Y. Effect of particle size in a colloidal hydrogel scaffold for 3D cell culture. *Colloids Surf. B* **2015**, *136*, 1139−1147.
(63) Zhang, S.-Z.; Lipsky, M. M.; Trump, B. F.; Hsu, I.-C. Neutral red (NR) assay for cell viability and xenobiotic−induced cytotoxicity in primary cultures of human and rat hepatocytes. *Cell Biol. Toxicol.* **1990**, *6*, 219−234.
(64) Zhao, F.; Zhou, X.; Shi, Y.; Qian, X.; Alexander, M.; Zhao, X.; Mendez, S.; Yang, R.; Qu, L.; Yu, G. Highly efficient solar vapour generation via hierarchically nanostructured gels. *Nat. Nanotechnol.* **2018**, *13*, 489−495.
(65) Li, X.; Ni, G.; Cooper, T.; Xu, N.; Li, J.; Zhou, L.; Hu, X.; Zhu, B.; Yao, P.; Zhu, J. Measuring conversion efficiency of solar vapor generation. *Joule* **2019**, *3*, 1798−1803.
(66) Yu, F.; Ming, X.; Xu, Y.; Chen, Z.; Meng, D.; Cheng, H.; Shi, Z.; Shen, P.; Wang, X. Quasimetallic molybdenum carbide−based flexible polyvinyl alcohol hydrogels for enhancing solar water evaporation. *Adv. Mater. Interfaces* **2019**, *6*, No. 1901168.
(67) Liang, X.; Zhang, X.; Liu, Z.; Huang, Q.; Zhang, H.; Liu, C.; Liu, Y. Direction−limited water transport and inhibited heat convection loss of gradient−structured hydrogels for highly efficient interfacial evaporation. *Sol. Energy* **2020**, *201*, 581−588.
(68) Yin, X.; Zhang, Y.; Guo, Q.; Cai, X.; Xiao, J.; Ding, Z.; Yang, J. Macroporous double-network hydrogel for high−efficiency solar steam generation under 1 sun illumination. *ACS Appl. Mater. Interfaces* **2018**, *10*, 10998−11007.
(69) Li, S.; He, Y.; Guan, Y.; Liu, X.; Liu, H.; Xie, M.; Zhou, L.; Wei, C.; Yu, C.; Chen, Y. Cellulose nanofibril−stabilized pickering emulsion and in situ polymerization lead to hybrid aerogel for high−efficiency solar steam generation. *ACS Appl. Polym. Mater.* **2020**, *2*, 4581−4591.
(70) Zhao, X.; Liu, C. Overcoming salt crystallization with ionic hydrogel for accelerating solar evaporation. *Desalination* **2020**, *482*, No. 114385.

https://doi.org/10.1021/acs.macromol.1c02129
Macromolecules XXXX, XXX, XXX−XXX